

First principles investigation of magnetocrystalline anisotropy at the $L2_1$ Full Heusler|MgO interfaces and tunnel junctions

Rajasekarakumar Vadapoo, Ali Hallal, Mairbek Chshiev
Univ. Grenoble Alpes, INAC-SPINTEC, F-38000 Grenoble, France
CNRS, SPINTEC, F-38000 Grenoble, France and
CEA, INAC-SPINTEC, F-38000 Grenoble
 (Dated: April 24, 2014)

Magnetocrystalline anisotropy at Heusler alloy|MgO interfaces have been studied using first principles calculations. It is found that Co terminated Co_2FeAl |MgO interfaces show perpendicular magnetic anisotropy upto 1.31 mJ/m^2 , while those with FeAl termination exhibit in-plane magnetic anisotropy. Layer resolved analysis indicates that the origin of perpendicular magnetic anisotropy in Co_2FeAl |MgO interfaces can be attributed to the out-of-plane orbital contributions of interfacial Co atoms. At the same time, Co_2MnGe and Co_2MnSi interfaced with MgO tend to favor in-plane magnetic anisotropy for all terminations.

Perpendicular magnetic anisotropy (PMA) in transition metal|insulator interfaces has been demonstrated more than a decade ago. [1, 2] These interfaces have become a viable alternative to PMA in fully metallic structures based on heavy non-magnetic elements with strong spin-orbit coupling (SOC) [3–6]. Indeed, high PMA values were observed in $\text{Co}(\text{Fe})|\text{MOx}$ ($\text{M}=\text{Ta}, \text{Mg}, \text{Al}, \text{Ru}$, etc.) interfaces despite their weak SOC [1, 2]. These structures serve as main constituents for perpendicular magnetic tunnel junctions (p-MTJ) which are very promising for realizing next generation of high density non volatile memories and logic devices [7–11]. One of the most important requirements for the use of p-MTJ in spintronic applications including high density spin transfer torque magnetic random access memory (STT-MRAM) is a combination of large PMA, high thermal stability and low critical current to switch magnetization of the free layer. CoFeB |MgO p-MTJ is one of the most promising candidates among state-of-the-art structures [10]. However, another class of ferromagnetic electrode materials with drastically improved characteristics for use in p-MTJ are Heusler alloys, since they possess much higher spin polarization [12] and significantly lower Gilbert damping [13].

Full Heusler alloys (X_2YZ)|MgO interfaces with high interfacial PMA and weak spin orbit coupling (SOC) have been gaining interest recently [12, 14–16]. For instance, MgO-based MTJs with Co_2FeAl (CFA) electrodes show high PMA in most of the experiments. The surface anisotropy energy (K_s) is found to be around 1 mJ/m^2 for Pt|CFA|MgO trilayer [17] and CFA|MgO [16, 18] interfaces. The observed PMA values for these structures are comparable to those reported for CoFeB|MgO [10] and tetragonally distorted $\text{Mn}_{2.5}\text{Ga}$ films grown on Cr buffered MgO [14]. However, there are reports on observation of in-plane magnetic anisotropy (IMA) for CFA|MgO interfacial structures in different cases [19, 20]. Thus, these interfaces show PMA with values between $0.16\text{--}1.04 \text{ mJ/m}^2$ [16, 21, 22] as well as IMA with $K_s=-1.8 \text{ mJ/m}^2$ [19]. On the other hand, some theoretical studies have reported PMA

values of 1.28 mJ/m^2 for Co terminated structures [23], IMA of 0.78 mJ/m^2 [23] and PMA of 0.428 mJ/m^2 [24] for FeAl termination. It has been suggested that interfacial Fe atoms are responsible for PMA in these structures [21] but the microscopic origins of anisotropy remains to be clarified further.

In order to elucidate the origin of PMA in these interfaces, we present a systematic study of magnetic anisotropy in Heusler alloy (X_2YZ)|MgO interfaces [with $\text{X}=\text{Co}$, $\text{YZ}=\text{FeAl}$, MnGe and MnSi] using first principles method. We explore the different interfacial conditions in these interfaces. In order to understand the microscopic mechanism of PMA, we employ the on-site projected and orbital resolved analysis of magnetocrystalline anisotropy energy (MA) which allows identification of layer contributions along with the corresponding different orbital contributions [25, 26]. We found that the magnetic anisotropy is much more complex compared to that in $\text{Co}(\text{Fe})|\text{MgO}$ structures [26] and it is strongly dependent on the interface termination and composition.

Calculations are performed using Vienna ab initio simulation package (VASP) [27, 28] with generalized gradient approximation [29] and projected augmented wave pseudopotentials [30, 31]. We used the kinetic energy cutoff of 600 eV and a Monkhorst-Pack k-point grid of $13 \times 13 \times 3$. Initially the structures were relaxed in volume and shape until the force acting on each atom falls below 1 meV/\AA . The Kohn-Sham equations were then solved to find the charge distribution of the ground state system without taking spin-orbit interactions (SOI) into account. Finally, the total energy of the system was calculated for a given orientation of magnetic moments in the presence of spin-orbit coupling. The surface magnetic anisotropy energy, K_s is calculated as $-1/a^2(E^\perp - E^\parallel)$, where a is the in-plane lattice constant and $E^\perp(E^\parallel)$ represents energy for out-of-plane(in-plane) magnetization orientation with respect to the interface. Positive and negative values of K_s corresponds to out-of-plane and in-plane anisotropy respectively. In addition, we define the effective anisotropy

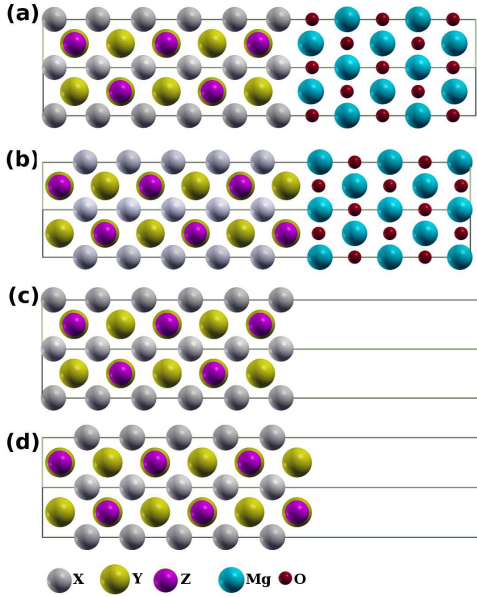


FIG. 1. (Color online) Perspective view of (a) X terminated, (b) YZ terminated interface structure of Heusler (X₂YZ)|MgO and (c) X terminated, (d) YZ terminated Heusler|Vacuum slabs with X=Co, YZ=FeAl, MnGe and MnSi. Grey, yellow, pink, blue and red spheres represent X, Y, Z, Mg and O atoms, respectively.

$K_{eff} = K_s/t_{CFA} - E_{demag}$, where E_{demag} is the demagnetization energy which is the sum of all the magnetostatic dipole-dipole interactions upto infinity. We adopt the dipole-dipole interaction method to calculate the E_{demag} term instead of $2\pi M_s^2$, where M_s is the saturation magnetization; since the latter underestimates this term for thin films. [26, 32]

Full-heusler (X₂YZ) alloys are intermetallic compounds with cubic $L2_1$ structure and belongs to the space group $Fm\bar{3}m$ [12, 33]. The magnetocrystalline anisotropy of bulk heusler is found to be negligible. The Heusler|MgO interfaces have been setup with the crystallographic orientation of Heusler(001)[100]||MgO(001)[110] [24, 34–36]. This results in a relatively low lattice mismatch between Heusler(001) and MgO(001) with a 45 degrees in-plane rotation. The energetically stable X and YZ terminations at the interface were studied and will be denoted as X-Heusler|MgO and YZ-Heusler|MgO as shown respectively in Fig. 1(a) and (b). The results of these interfaces will be compared to those of X-Heusler|Vacuum and YZ-Heusler|Vacuum slabs shown in Fig. 1(c) and (d), respectively.

Increasing the MgO thickness beyond 5 monolayers (ML) is found to have no effect on magnetic anisotropy. The variation of surface magnetic anisotropic energy (K_s) with the thickness of Heusler layers varying from 3 to 11 ML for the Heusler|MgO interfaces is shown in Fig. 2. One can see that only Co-CFA|MgO structure gives rise to very high PMA which weakly de-

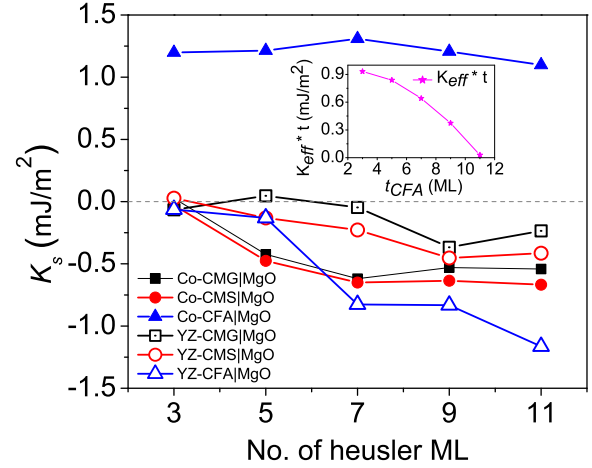


FIG. 2. (Color online) Surface magnetic anisotropy energy (K_s) as a function of number of heusler monolayers (ML) in Co and YZ terminated heusler (X₂YZ)|MgO structures. Filled data points represent Co terminated and open data points represent YZ terminated interfaces. Blue triangle represent Co₂FeAl (CFA), black square for Co₂MnGe (CMG) and red circle for Co₂MnSi (CMS) interfaces. Inset shows the effective anisotropy ($K_{eff} * t$) as a function of thickness of CFA in Co terminated CFA|MgO interface.

pend on CFA thickness, while the FeAl-CFA|MgO and all CMG|MgO as well as CMS|MgO show IMA. It is interesting to note that the magnetic anisotropy energy for the CMG|MgO and CMS|MgO as a function of thickness follow similar trend which might be due to the inert nature of Z-element (Ge, Si). The in-plane anisotropy contribution in these structures increases as a function of thickness and stabilizes after 9 ML. It can be seen that K_s for Co-CFA|MgO increases from 1.20 mJ/m² to a maximum of 1.31 mJ/m² at 7 ML thickness (~ 0.8 nm), which is in agreement with experimental findings of M. S. Gabor et al. [22] and Z. Wen et al. [16]. Inset in Fig. 2 shows the corresponding effective anisotropy ($K_{eff} * t$) as a function of CFA thickness (t_{CFA}). It shows a decaying behavior and vanishes around 11 ML becoming IMA beyond this thickness, in reasonable agreement with recent experiments [16, 22].

In order to understand the origin of PMA and effect of MgO, we examined the on-site projected magnetic anisotropy for the 11 ML of Heusler|MgO and their free surface counterparts as shown in Fig. 3. As one can see, the major PMA contribution of 0.69 mJ/m² in Co-CFA|MgO structure comes from the interfacial Co atoms while the inner layers show fair amount of in-plane or out-of-plane contributions represented by solid pink bars in Fig. 3(a). By comparing with CFA|Vacuum shown by unfilled pink bars in the same figure, we can clearly identify that the presence of MgO on top of Co layer plays a decisive role in establishing the PMA in Co terminated CFA|MgO structure. More complicated behavior is observed for Co-CMG and Co-CMS structures

where the role of MgO in anisotropy varies depending on layer. While it tends to decrease(increase) the IMA in the 1st Co layer for Co-CMG(Co-CMS), it simultaneously flips the IMA into PMA (PMA into IMA) for 2nd YZ (3rd Co) layer.

Similar nontrivial picture is observed for YZ terminated CMG and CMS structures shown in Fig. 3(b). By employing the same analysis in order to clarify the role of MgO vs vacuum next to YZ terminated Heusler alloy, one can see that the MgO has a tendency to improve the IMA for the case of YZ-CFA for all layers, it enhances the PMA(IMA) for the 1st(2nd and all Co) layers of YZ-CMS and YZ-CMG structures. Overall it can be concluded that in all cases Co layers favor IMA except the interfacial layer in Co-CFA and Co-CMG structures while inner YZ layers in most cases tend to favor the PMA. In addition, YZ interfacial layer favor the IMA(PMA) for YZ-CFA(YZ-CMS and YZ-CMG).

To further elucidate the microscopic origin of PMA, we carried out the d -orbital resolved magnetic anisotropy contributions for interfacial atoms as shown in Fig. 4. One can see that the switch from IMA to PMA when MgO is placed on top of Co terminated CFA mainly arises from the out-of-plane orbitals ($d_{xz, yz}$ and d_{z^2}) as shown by comparison of XV and XM columns in Fig. 4(a). Furthermore, this switch is assisted by all d orbitals within the 2nd (YZ) layer. At the same time, the MgO-induced enhancement of the IMA in the first two layers from interface (FeAl and Co) in case of YZ terminated CFA (see Fig. 3(b)) is due to increase(decrease) of IMA(PMA) contribution from $d_{x^2-y^2}$ (d_{yz} and d_{z^2}) orbitals, as seen from comparison of columns YV and YM in Fig. 4(a).

In the case of Co terminated CMG, the effect of MgO results in overall tendency to decrease the IMA with participation of in-plane d orbitals (d_{xy} and $d_{x^2-y^2}$) in the first Co layer with a quite interesting opposing contributions from out-of-plane d_{yz} and d_{z^2} orbitals (see XV and XM columns in Fig. 4(b)). At the same time, for the second layer (MnGe) contribution, the presence of MgO has a clear tendency to switch from IMA into PMA assisted by all d -orbitals. As for Mn terminated CMG, the presence of MgO has almost no effect on 1st MnGe layer anisotropy contributions, while it induces the flip from PMA to IMA from almost all d orbitals within the second Co layer (Fig. 4(b)). The orbital contributions for CMS are found to be very similar to CMG orbital contributions.

Aforementioned analysis shows that Co-CFA|MgO structure favors the high PMA while YZ termination in CFA|MgO structure give rise to IMA. This allows us to conclude that interfacial Co atoms are responsible for the PMA. However, it was claimed recently that the origin of PMA could be attributed to Fe atoms at the interface in CFA|MgO [21] using XMCD measurements in combination with Bruno's model analysis [37]. In order

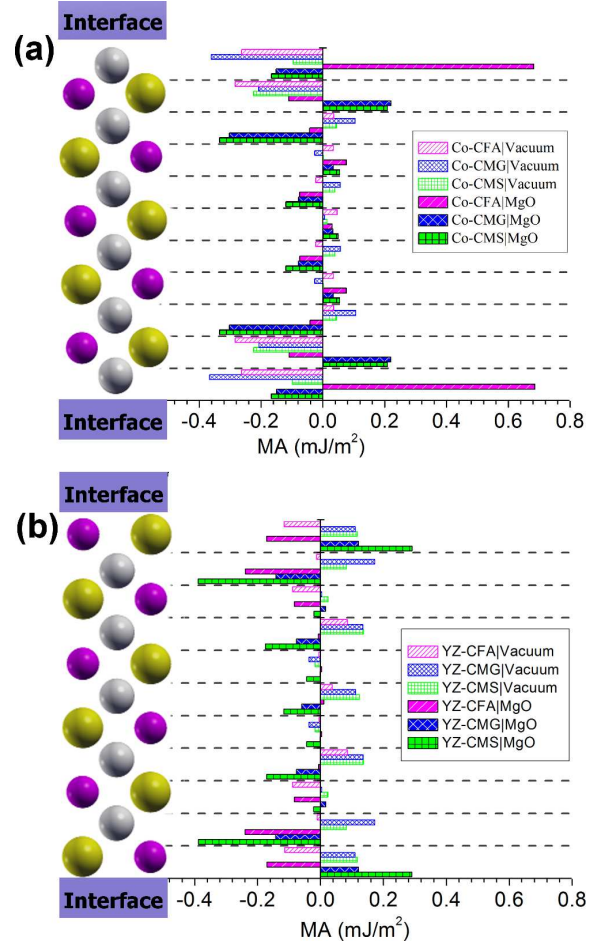


FIG. 3. (Color online) Onsite projected magnetic anisotropy for (a) Co terminated and (b) YZ terminated heusler (X_2YZ [Co_2FeAl (CFA), Co_2MnGe (CMG) and Co_2MnSi (CMS)]|MgO interfaces and its free surfaces. Sparse pattern with solid fill represents Heusler|MgO and dense unfilled pattern represents Heusler|Vacuum structures. Pink, blue and green colors represent CFA, CMG and CMS structures respectively. The structure of the corresponding Heusler (X_2YZ) monolayers are shown on the left for both Co and YZ terminations. The atomic elements X, Y and Z are represented by grey, yellow and pink spheres respectively.

to resolve this disagreement, we carried out the orbital momentum calculations for 7 ML structure corresponding to that reported in experiments [21] with both terminations. We systematically found that per layer resolved orbital moment anisotropy (OMA) is inconsistent with layer resolved MA contributions for Co layers while it remains in qualitative agreement for layers containing Fe. We can therefore conclude that Bruno's model should be used with caution and its validity may depend on particular system.

In summary, using first principles calculation we investigated the magnetic anisotropy of Full Heusler|MgO interfaces and MTJs for all terminations. It is found that Co terminated CFA|MgO shows the PMA

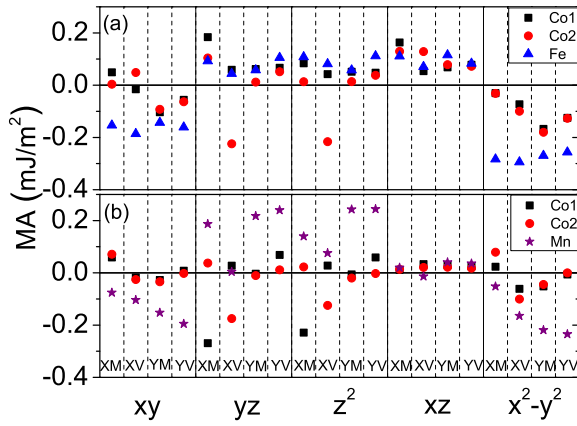


FIG. 4. (Color online) d -orbital resolved contribution to magnetic anisotropy for interfacial atoms in Co-terminated and YZ-terminated interfaces of (a) $\text{Co}_2\text{FeAl}|\text{MgO}$ and (b) $\text{Co}_2\text{MnGe}|\text{MgO}$ and their free surfaces. Black square and red circle represents the Co atoms. Blue triangle and purple star represent Fe and Mn atom contributions respectively. XV, XM, YV and YM represent Co-Heusler|Vacuum, Co-Heusler|MgO, YZ-Heusler|Vacuum and YZ-Heusler|MgO interfaces respectively.

of 1.31mJ/m^2 induced by the presence of MgO in agreement with recent experiments while FeAl terminated CFA and other structures possess the IMA. We also unveiled the microscopic mechanisms of PMA in Heusler|MgO structures by evaluating the onsite projected and orbital resolved contributions to magnetic anisotropy and found that interfacial Co atoms are responsible for high PMA (IMA) in CFA (CMG,CMS). Finally, out-of-plane (in-plane) orbitals tend to favor mainly PMA (IMA).

The authors thanks H.-X. Yang and C. Tiusan for fruitful discussions. This work was partly supported by French ANR SPINHALL and SOSPIN projects.

- [1] S. Monso, B. Rodmacq, S. Auffret, G. Casali, F. Fetta, B. Gilles, B. Dieny, and P. Boyer, Appl. Phys. Lett. **80**, 4157 (2002).
- [2] B. Rodmacq, S. Auffret, B. Dieny, S. Monso, and P. Boyer, J. Appl. Phys. **93**, 7513 (2003).
- [3] N. Nakajima, T. Koide, T. Shidara, H. Miyauchi, H. Fukutani, A. Fujimori, K. Iio, T. Katayama, M. Nývlt, and Y. Suzuki, Phys. Rev. Lett. **81**, 5229 (1998).
- [4] P. F. Carcia, A. D. Meinhardt, and A. Suna, Appl. Phys. Lett. **47**, 178 (1985).
- [5] H. J. G. Draaisma, W. J. M. de Jonge, and F. J. A. den Broeder, J. Magn. Magn. Mater. **66**, 351 (1987).
- [6] D. Weller, Y. Wu, J. Stöhr, M. G. Samant, B. D. Hermsmeier, and C. Chappert, Phys. Rev. B **49**, 12888 (1994).
- [7] G. Kim, Y. Sakuraba, M. Oogane, Y. Ando, and T. Miyazaki, Appl. Phys. Lett. **92**, 172502 (2008).

- [8] L. E. Nistor, B. Rodmacq, S. Auffret, and B. Dieny, Appl. Phys. Lett. **94**, 012512 (2009).
- [9] L. E. Nistor, B. Rodmacq, S. Auffret, A. Schuhl, M. Chshiev, and B. Dieny, Phys. Rev. B **81**, 220407 (2010).
- [10] S. Ikeda, K. Miura, H. Yamamoto, K. Mizunuma, H. D. Gan, M. Endo, S. Kanai, J. Hayakawa, F. Matsukura, and H. Ohno, Nature Mater. **9**, 271 (2010).
- [11] M. Endo, S. Kanai, S. Ikeda, F. Matsukura, and H. Ohno, Appl. Phys. Lett. **96**, 212503 (2010).
- [12] T. Graf, C. Felser, and S. S. Parkin, Prog. Solid State Chem. **39**, 1 (2011).
- [13] C. Liu, C. K. A. Mewes, M. Chshiev, T. Mewes, and W. H. Butler, Appl. Phys. Lett. **95**, 022509 (2009).
- [14] F. Wu, S. Mizukami, D. Watanabe, H. Naganuma, M. Oogane, Y. Ando, and T. Miyazaki, Appl. Phys. Lett. **94**, 122503 (2009).
- [15] W. Wang, H. Sukegawa, and K. Inomata, App. Phys. Express **3**, 093002 (2010).
- [16] Z. Wen, H. Sukegawa, S. Mitani, and K. Inomata, Appl. Phys. Lett. **98**, 242507 (2011).
- [17] X. Li, S. Yin, Y. Liu, D. Zhang, X. Xu, J. Miao, and Y. Jiang, Appl. Phys. Express **4**, 043006 (2011).
- [18] Y. Cui, B. Khodadadi, S. Schaäfer, T. Mewes, J. Lu, and S. a. Wolf, Appl. Phys. Lett. **102**, 162403 (2013).
- [19] M. Belmeguenai, H. Tuzcuoglu, M. S. Gabor, T. Petrisor, C. Tiusan, D. Berling, F. Zighem, T. Chauveau, S. M. Chèrif, and P. Moch, Phys. Rev. B **87**, 184431 (2013).
- [20] M. Belmeguenai, H. Tuzcuoglu, M. S. Gabor, T. Petrisor, C. Tiusan, D. Berling, F. Zighem, T. Chauveau, S. M. Chèrif, J. Magn. Magn. Mater. (In press).
- [21] J. Okabayashi, H. Sukegawa, Z. Wen, K. Inomata, and S. Mitani, Appl. Phys. Lett. **103**, 102402 (2013).
- [22] M. S. Gabor, T. Petrisor, and C. Tiusan, J. Appl. Phys. **114**, 063905 (2013).
- [23] M. Tsujikawa, D. Mori, Y. Miura, and M. Shirai, MML2013- 8TH International Symposium on Metallic Multilayers Mo-8, (2013).
- [24] Z. Bai, L. Shen, Y. Cai, Q. Wu, M. Zeng, G. Han, and Y. P. Feng, cond-mat-mtrl-sci, arXiv:1303.3473 (2013).
- [25] H. X. Yang, M. Chshiev, B. Dieny, J. H. Lee, A. Manchon, and K. H. Shin, Phys. Rev. B **84**, 054401 (2011).
- [26] A. Hallal, H. X. Yang, B. Dieny and M. Chshiev, Phys. Rev. B **88**, 184423 (2013).
- [27] G. Kresse, and J. Hafner, Phys. Rev. B **47**, 558 (1993).
- [28] G. Kresse, and J. Furthmuller, Phys. Rev. B **54**, 11169 (1996).
- [29] Y. Wang, and J. P. Perdew, Phys. Rev. B **44**, 13298 (1991).
- [30] G. Kresse, and D. Joubert, Phys. Rev. B **59** 1758 (1999).
- [31] P. E. Blöchl, Phys. Rev. B **50**, 17953 (1994).
- [32] G. H. O. Daalderop, P. J. Kelly, and M. F. H. Schuurmans, Phys. Rev. B **41**, 11919 (1990).
- [33] C. a. Culbert, M. Williams, M. Chshiev, and W. H. Butler, J. Appl. Phys. **103**, 07D707 (2008).
- [34] M. Yamamoto, T. Marukame, T. Ishikawa, K. Matsuda, T. Uemura, and M. Arita, J. Phys. D: Appl. Phys. **39**, 824 (2006).
- [35] M. S. Gabor, T. Petrisor, C. Tiusan, M. Hehn, T. Petrisor, Phys. Rev. B **84**, 134413 (2011).
- [36] A. Grünebohm, H. C. Herper, M. E. Gruner, and P. Entel, IEEE Transactions on magnetics **49**, 3965 (2009).
- [37] P. Bruno, Phys. Rev. B **39**, 865 (1989).